Australian Meteorological and Oceanographic Journal 63 (2013) 265–284

Implementation of the initial ACCESS numerical weather prediction system

K. Puri, G. Dietachmayer, P. Steinle, M. Dix, L. Rikus, L. Logan, M. Naughton, C. Tingwell, Y Xiao, V. Barras, I. Bermous, R. Bowen, L. Deschamps, C. Franklin, J. Fraser, T. Glowacki, B. Harris, J. Lee, T. Le, G. Roff, A. Sulaiman, H. Sims, X. Sun, Z. Sun, H. Zhu, M. Chattopadhyay, C. Engel

Centre for Australian Weather and Climate Research,
A partnership between CSIRO and the Bureau of Meteorology

(Manuscript received June 2012; revised December 2012)

The Australian Community Climate and Earth-System Simulator (ACCESS) is a coupled climate and earth system simulator being developed as a joint initiative of the Bureau of Meteorology and CSIRO in cooperation with the university community in Australia. The main aim of ACCESS is to develop a national approach to climate and weather prediction model development. Planning for ACCESS development commenced in 2005 and significant progress has been made subsequently. ACCESS-based numerical weather prediction (NWP) systems were implemented operationally by the Bureau in September 2009 and were marked by significantly increased forecast skill of close to one day for three-day forecasts over the previously operational systems. The fully-coupled ACCESS earth system model has been assembled and tested, and core runs have been completed and submitted for the Intergovernmental Panel for Climate Change (IPCC) Fifth Assessment Report. Significant progress has been made with ACCESS infrastructure including successful porting to both Solar and Vayu (National Computational Infrastructure (NCI)) machines and development of infrastructure to allow usage by university researchers. This paper provides a description of the NWP component of ACCESS and presents results from detailed verification of the system.

Introduction

The Australian Community Climate and Earth System Simulator (ACCESS) is a fully coupled earth system model (ESM) being jointly developed by the Bureau of Meteorology and CSIRO, with help from the Australian universities. A key aim of ACCESS is to develop a system that enables a national approach to climate and weather prediction model development, and will also provide the Bureau and CSIRO the capability to underpin Australia's basic weather and climate services and to conduct the best possible science for use in analysing climate impacts and adaptation. ACCESS will also enable Australian scientists to contribute to major international model intercomparison projects and provide opportunities for scientists to share knowledge, form collaborations and initiate new projects.

ACCESS planning started in 2005 with the development of two key documents, namely: 'Blueprint for ACCESS' (K. Puri, June 2005, available at http://www.cawcr.gov.au/staff/kkp/ACCESS/access_blueprint.pdf) and 'Project Plan for ACCESS' (K. Puri, September 2005, available at http://www.cawcr.gov.au/staff/kkp/ACCESS/access_project_plan.pdf)

The 'Blueprint' provided an analysis of ACCESS stakeholder requirements and developed the scope for ACCESS, based on these requirements and an analysis of earth system models in use at a number of key international centres. The 'Project Plan' provided the scientific justification for ACCESS and recommendations for the preferred options for the components, together with an estimate of the level of investment required for ACCESS to achieve its required objectives. Development of ACCESS has followed the recommendations made in the project plan with significant collaboration with international partners, particularly the UK Met Office.

ACCESS is designed to provide a seamless modelling system, based on the concept of a continuum of prediction problems, with a blurring of the distinction between shorter-term predictions and longer-term climate predictions, and brings together multi-disciplinary strengths across disciplines ranging from modelling, data assimilation

Corresponding author address: K. Puri, CAWCR, Bureau of Meteorology, GPO Box 1289 Melbourne Vic. 3001. Email: k.puri@bom.gov.au

and software engineering. Table 1 shows the final agreed components of ACCESS and the source of individual modules. Figure 1 shows a schematic of the fully coupled ACCESS. All subsequent work has been aimed at completing development of the fully coupled system depicted in the schematic. Note that the ocean and sea-ice modules are coupled to the atmospheric model via the OASIS coupler as the modules use different grids and resolutions; the land-surface and chemistry modules on the other hand are coupled directly to the atmospheric model as they are on the same grid although this could change in the future.

The fully-coupled ACCESS has now been technically assembled, and core runs in climate mode have been completed and submitted for consideration for the Intergovernmental Panel for Climate Change (IPCC) Fifth Assessment Report. A major milestone in the ACCESS development was reached in September 2009 when the numerical weather prediction component (atmospheric model + land surface model + data assimilation) was implemented operationally by the Bureau of Meteorology's National Meteorological and Oceanographic Centre (NMOC).

This paper provides a description of the numerical weather prediction (NWP) system and presents some results to provide an indication of the performance of the ACCESS NWP system. The fully-coupled model implementation has been described in Bi et al. (2013).

Fig. 1. Schematic for the target ACCESS system for climate/climate change applications and for NWP applications.

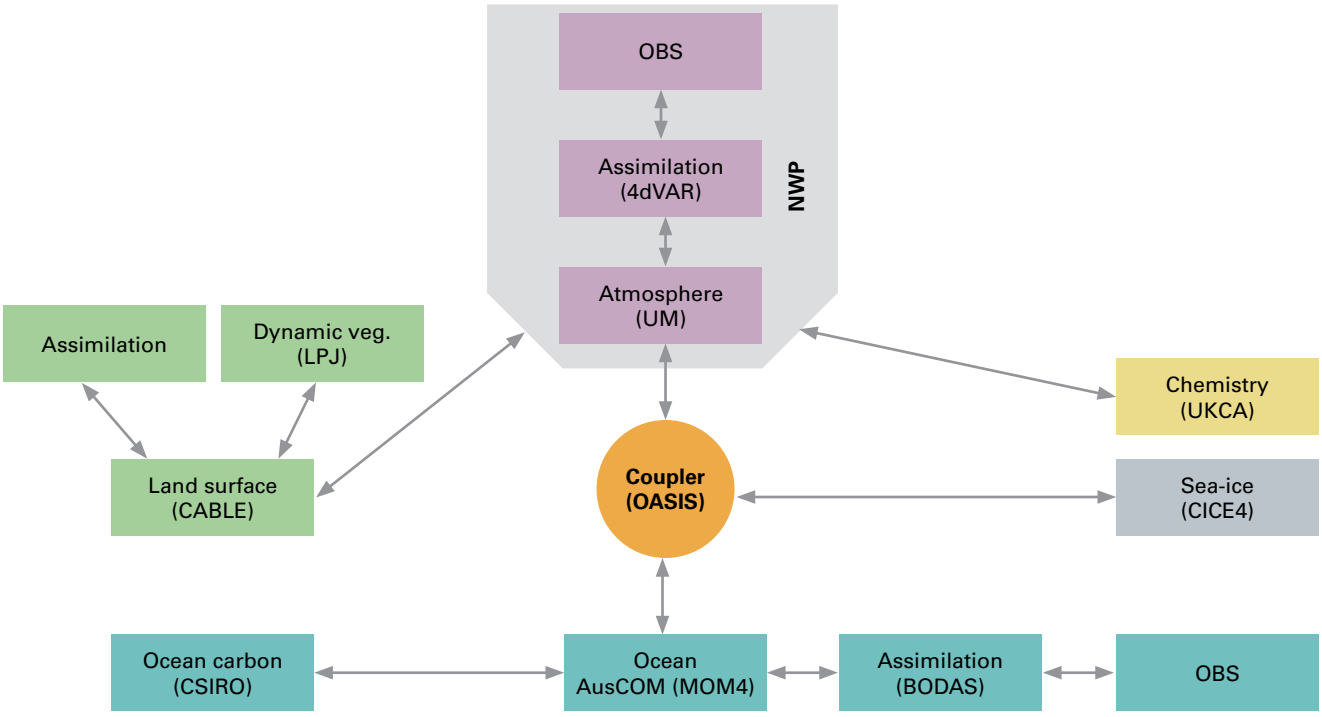

Table 1. Modules of the ACCESS ESM.

Module	*Name*	*Source*
Atmosphere	Met Office Unified Model (UM)	MetOffice
Ocean	Modular Ocean Model version 4 (MOM4)	NOAA Geophysical Fluid Dynamics Laboratory
Sea-ice	The Los Alamos Sea Ice Model version 4 (CICE4)	Department of Energy Los Alamos National Laboratory
Land surface/carbon cycle	The CSIRO Atmosphere Biosphere Land Exchange model (CABLE)	CSIRO
Chemistry and aerosols	United Kingdom Chemistry and Aerosol model (UKCA)	UK Met Office, Leeds and Cambridge universities
Data Assimilation – atmosphere	4-dimensional variational assimilation (4dVAR)	MetOffice
Data Assimilation – ocean	Ensemble Kalman Filter	Bureau/CSIRO
Coupler	OASIS	CERFACS (Centre Européen de Recherche et de Formation Avancée en Calcul Scientifique)

Description of NWP component

Two key recommendations made by Puri (Project Plan for ACCESS, September 2005) were:

'ACCESS should import the Met Office atmospheric model HadGAM1 to provide the initial atmospheric model for ACCESS'; and

'The Met Office 4dVAR scheme should be imported to form the atmospheric data assimilation module in ACCESS'.

The Met Office Unified Model (UM) and data assimilation system (OPS/VAR) have been obtained under a research licence signed between the Bureau, CSIRO and the Met Office. The sections below present an overview of UM/VAR systems.

Unified Model (UM) formulation

Detailed descriptions of the UM dynamical core and physical parametrisations can be found in Davies et al. (2005) and Cullen (1993) and only a brief description will be given here. The initial NWP implementation used version 6.4 of the UM in keeping with the Met Office operational system.

Dynamics

The UM is applied across all length scales, hence its dynamical core (DC) is built around a nonhydrostatic formulation. The DC has no 'hydrostatic option'; it always runs including nonhydrostatic effects, even for climate simulations. This approach is made computationally feasible by careful choice of time-stepping algorithms (see below). Many hydrostatic models, including the Bureau 'LAPS' system, use pressure-based coordinate-transforms to facilitate the inclusion of topography. It is possible to extend this approach to nonhydrostatic models (Laprise 1992), but the UM DC uses a transformed geometric-height coordinate, as has been adopted in small-scale models for some time now (Clark 1977). Thus, in contrast to previous Bureau operational NWP models, the UM grid-points are fixed in space, and do not move vertically in response to pressure variations.

In a dry nonhydrostatic DC we require fully prognostic equations to represent the conservation of momentum, mass, and energy. In the UM DC the related prognostic variables are u, v, and w (the zonal, meridional and vertical winds), density (specifically, the mass of dry air per unit volume of moist air), and potential-temperature. Moist processes are supported by the introduction of additional prognostic variables for the mixing-ratios of water-vapour, cloud-liquid-water, and cloud-frozen-water, all taken with respect to dry air. In terms of the grid layout of the variables, an Arakawa-C grid (Arakawa and Lamb 1977) is used in the horizontal, and a Charney-Phillips scheme in which thermodynamic and moisture variables are stored on model half-levels is used in the vertical (Charney and Phillips 1953).

With exceptions noted later, the prognostic equations are advanced in time using a two time-level, semi-implicit, semi-Lagrangian (SL) scheme which, by design, allows for the stable use of large model time-steps (see Staniforth et al. 2006 for details). 'Orographic resonance', an instability associated with the use of SL schemes in the presence of significant topography (Rivest et al. 1994), is avoided using the standard approach of backward time-weighting of the implicit terms.

The UM DC supports a wide range of interpolation options for the calculation of field values at SL 'departure points', and these can be applied on a per-field basis. The higher-order schemes can be combined with a nonlinear monotonicity-preserving option, using the method of Bermejo and Staniforth (1992). In the current operational implementation, the high-order scheme used is cubic Lagrange interpolation, and monotonicity is enforced for temperature and moisture.

SL schemes require evaluation of backward trajectories, which poses some challenges in spherical (lat/lon) coordinates. In the UM, a modified (two time-level versus three) version of the computationally efficient Ritchie and Beaudoin (1994) scheme is used over most of the domain, but near the poles, where coordinate distortion becomes increasingly difficult to handle, a local rotated pole scheme is used, along the lines of McDonald and Bates (1989).

There are exceptions to the time-stepping process described above. First, given both the primacy of mass conservation, and the relative meteorological unimportance of acoustic modes, the prognostic density equation is formulated using an implicit, Eulerian (flux-form) scheme. Second, for stability reasons, a non-interpolating SL scheme is used to model the vertical advection of temperature.

In contrast to previous Bureau NWP systems, the current operational implementation of the UM has no all-of-domain horizontal diffusion applied, though local, 'targeted diffusion' of moisture is applied whenever the vertical velocity exceeds some critical value (which is taken as being indicative of a 'grid-point-storm').

Application of the time-advancement algorithm described above is formulated as a number of steps, which varies dependent on the particular variable. For example, for u there are two physics steps (one for fast processes such as boundary layer and convective transport, and one for slow processes such as radiation), and a number of dynamics predictor-corrector steps, which, due to the semi-implicit treatment used, couple the prognostic equations together. This coupled set can be reduced to a single Helmholtz equation for the Exner pressure tendency, which is solved using a preconditioned generalised conjugate residual method.

Physical parametrisations

A detailed description of the parametrisations used in the UM is given in Walters et al. (2011). Key features include:

Clouds

The 6.4 version of the UM simulates clouds using the diagnostic scheme of Smith (1990). This scheme is based on two 'cloud-conserved' variables: T_L, the 'liquid-frozen water temperature' (the temperature obtained by evaporating all the cloud water in the grid-box), and q_T, the total water content in a grid-box. A particular probability distribution of the sub-grid scale perturbations of these variables is assumed, from which the cloud amounts and water contents are derived using an assumed critical relative humidity. The scheme is modified such that only water clouds are defined from T_L and q_T and a sub-grid probability distribution. Ice water content is determined by the prognostic mixed phase microphysics scheme with ice cloud fraction calculated diagnostically from ice water content. An additional parametrisation to derive cloud area is included, where the approach is to interpolate T_L and q_T to higher effective vertical resolution and use the cloud scheme on these interpolated levels. The cloud on these sub-layers is assumed to be maximally overlapped so that the area cloud fraction that is seen by the radiation scheme is given by the maximum of the sub-layer values of the volume cloud fraction.

Radiation

The radiation scheme developed by Edwards and Slingo (1996) is used in the ACCESS model. The scheme utilises a correlated-k distribution method to parameterise the transmittance of the atmospheric absorbing gases and the two-stream approximation to solve the radiative transfer equations. It has six short-wave spectral bands and eight long-wave bands. Apart from the effects of H_2O, CO_2, and O_3 it also includes the effects of O_2, N_2O, CH_4, CFC11, CFC12. The code has a flexible spectral framework which suits both applications for high-resolution narrow band models for research purposes and low-resolution broad band models for NWP and climate models. Cloud ice crystals and water droplets are treated separately in the scheme. An ice cloud optical property scheme representing various non-spherical ice crystals developed by Edwards et al. (2007) is used in the current version of ACCESS model.

Boundary layer

Turbulent fluxes of heat, moisture and horizontal momentum in the boundary layer are represented by a first-order K profile closure as described by Lock et al. (2000).

The non-local part of the scheme checks for the presence of clear and cloudy unstable layers using a parcel ascent-descent method and uses this to classify the boundary layer into one of seven categories with a characteristic mixing profile. These are then adjusted with respect to the surface and cloud-top driven fluxes.

For stable conditions, the mixing length scheme of Louis (1979) is used to determine the mixing profile in terms of the local Richardson Number (Ri). At values of $Ri > 0$, the model uses alternate forms of the stability functions which allow for different degrees of mixing over the land and the ocean. Over land, the Louis 'long-tailed' function is used which allows for a slightly greater degree of mixing in order to accommodate heterogeneities on the sub-grid scale, whereas over the ocean the model uses the SHARPEST functions (King et al. 2001, Edwards et al. 2006) which inhibit mixing more rapidly at higher stabilities.

In addition to the explicit calculations described above, the ACCESS PBL scheme also uses an implicit numerical solver to determine the fluxes at the land–atmosphere interface. Within each time step, an initial increment of temperature and humidity is calculated for each model level. Surface fluxes are then corrected to remain consistent with the land surface energy balance. Finally, a readjustment is made to the initial increments of the atmosphere temperature and humidity profiles to bring them in line with the derived surface flux.

Precipitation

The Wilson and Ballard (1999) single-moment bulk microphysics scheme is used in the UM with explicit calculation of transfers between vapour, liquid and ice phases. The one ice water prognostic variable is split by a diagnostic relationship into ice crystals and aggregates, which are treated separately in the microphysical transfer terms before being recombined after the calculations. The microphysical processes calculated in the scheme are: sedimentation of ice and rain, heterogeneous and homogeneous nucleation of ice particles, deposition and sublimation of ice, aggregation, riming and melting of ice, collection of cloud droplets by raindrops, auto-conversion and accretion production of raindrops, and evaporation of rain (condensation and evaporation of cloud water is performed by the cloud scheme).

Convection

The convection scheme currently used in the UM is a modified mass flux scheme based on Gregory and Rowntree (1990).

Initiation of convection is based on evaluation of undiluted parcel ascent from the near surface, which is used to determine whether convection is possible from the boundary layer. Categorisation of convection as deep or shallow depends on the level of the cloud top. The mid-level convection scheme operates on any instabilities found in a column above the top of the shallow convection or above the boundary layer in columns where the surface layer is stable.

For deep convection, the cloud-base mass-flux is calculated based on the reduction to zero of convectively available potential energy (CAPE) over a given timescale. The CAPE closure has been modified in various ways to try to address model stability concerns (grid-point storms), with the vertical velocity based CAPE closure the option used in most model configurations. In this scheme the CAPE timescale is reduced to remove convective instability more rapidly if the maximum large-scale vertical velocity, evaluated before convection, is larger than a given threshold

vertical velocity. For deep convection, entrainment is based on prescribed profiles. Mixing detrainment rates depend on relative humidity and an adapted detrainment scheme is used to calculate the forced detrainment rates. The representation of convective momentum transports (CMT) is based on an eddy viscosity model, and a flux gradient approach has been introduced in the latest version of model.

The shallow convection scheme can produce precipitation, and the cloud-base mass-flux is proportional to the sub-cloud convective velocity scale, with separate entrainment and detrainment rates based on similarity theory. The shallow convective momentum transport uses a turbulence based CMT scheme based on cloud resolving model (CRM) simulations of shallow convection.

The mid-level scheme closely resembles the original Gregory-Rowntree mass flux scheme and uses a CAPE closure. The entrainment and detrainment rates are similar to those of the deep convection scheme.

Gravity wave drag

The gravity wave drag scheme includes an orographic gravity wave scheme (Webster et al. 2003, Webster 2004) and a spectral gravity wave scheme (Warner and McIntyre 1996, 1999, 2001, Warner et al. 2005, Bushell et al. 2007). The orographic gravity wave scheme allows for blocking as well as gravity wave drag and has been shown to improve the general circulation (McFarlane 1987, Webster et al. 2003). Similarly, the spectral scheme has been shown to improve tropical stratospheric simulations (Scaife et al. 2000, 2002).

In the orographic scheme the surface stress accounts for the anisotropy of the sub-grid orography and is then partitioned between blocked flow and linear hydrostatic gravity wave components dependent on the low-level Froude number. The former is then deposited uniformly over the lower levels while the latter is deposited aloft according to wave saturation theory. Note that the drag is not applied above 40 km in order to prevent unrealistically large drags being applied.

The spectral scheme is the Ultra-Simple Spectral Parameterisation (USSP) scheme and it treats non-orographic gravity waves with non-zero phase speeds by launching an unsaturated spectrum isotropically along the four cardinal directions from a level close to the surface and then calculating the total flux at a particular height by allowing for Doppler shifting and saturation effects. The model top is treated as transparent and allows the residual pseudomomentum to pass out of the model.

Land surface interaction

The Met Office Surface Exchange Scheme version 2 (MOSES2; Essery et al. 2001) soil is discretised into four layers of 0.1, 0.25, 0.65 and 2 m thickness from top to bottom. MOSES2 uses a tiled representation of heterogeneous surfaces. There are five vegetation tiles (broadleaf trees, needleleaf trees, temperate grasses, tropical grasses and shrubs) and four non-vegetation tiles (bare soil, open water, land ice and urban). The grid-box tile fractions are derived from the International Geosphere Biosphere Programme (IGBP) global land cover dataset. Transpiration by plants extracts soil water directly from the soil layers via the plant roots while bare soil evaporation extracts soil water from the top soil layer only. The ability of plants to access water from each soil layer is determined by the root density distribution and soil moisture availability. The broadleaf trees are assumed to have a root depth of 3 m, needleleaf trees 1 m, and grasses and shrubs 0.5 m. MOSES2 allows bare soil evaporation to occur even when the surface soil moisture is below the wilting point (see equation 35 of Essery et al. 2001). This means that in arid regions, the MOSES2 surface soil moisture can fall significantly below the wilting point.

The soil hydrology is based on a finite difference form of the Richards equation and Darcy's law. The Campbell (1974) equations are used to describe the relationship of soil hydraulic conductivity and soil suction to the unfrozen volumetric soil moisture. The soil hydraulic properties are calculated from the soil texture (sand, silt and clay fractions) using the regression relationships derived by Cosby et al. (1984). Three soil texture types (coarse, medium and fine) are allowed and the $1° \times 1°$ soil texture map of Wilson and Henderson-Sellers (1985) is used. The soil thermodynamics are represented by diffusive heat exchanges between the soil layers and by heat advection between the soil layers by the fluxes of moisture. The freezing and melting of soil water are also represented and the associated latent heat is included in the thermodynamic calculations. The calculation of the MOSES2 soil thermal capacity and heat conductivity are described by Appendix B of Cox et al. (1999).

The global model uses grid-box averages of the tile properties so that only a single energy balance equation is solved at each land surface column (this is referred to as the one tile option). The Met Office soil moisture nudging scheme (Best and Maisey 2002) is only used with the one tile version of MOSES2 since the nudging scheme requires the grid-box average tile properties as input. The regional models use the full tiling scheme which is computationally more expensive.

Assimilation (VAR)

There have been major developments in the past 20 years in the science and implementation of analysis methods, leading to the operational implementation of four-dimensional variational algorithms (4dVAR) and research on Kalman filter assimilation algorithms. These developments provide the capability of assimilating data from a wide range of observation systems, and particularly from satellites, and have resulted in significant improvements in short- and medium-range weather prediction.

The Met Office system (VAR) used in ACCESS includes a comprehensive analysis system using a variational scheme that incorporates both 3dVAR and 4dVAR and is designed for use in both global and limited area models. The 4dVAR

system includes perturbation forecast and adjoint models to provide explicit representation of the time dimension with a six-hour data window.

Key features of the assimilation system include the observation processing system (OPS), quality control, variational assimilation, linear model and adjoint and initialisation. Full details of the system are described in Rawlins et al. (2007) and only an overview is provided here. Key components include:

OPS and observation input

The observation processing system (OPS) uses most routinely available in situ and remotely sensed data, and substantially more than earlier Bureau operational systems GASP and LAPS. Significant modifications were required of the OPS to generalise the source of observations. The interface (between the Bureau database and OPS) of choice was based on the Observation Data Base (ODB) from the European Centre for Medium-range Weather Forecasting. This provides a flexible method of storing observations data encoded in the Binary Universal Form for the Representation of meteorological data (BUFR) that can then be efficiently accessed in parallel on many platforms. This interface also admits the possibility of efficient writing of quality control information and thence the detailed monitoring of all observations. Use of the ODB in interfacing observations marks a key difference between ACCESS and the Met Office system (see Fig. 4).

Available measurements of screen temperature and relative humidity, 10 m winds and station level pressure from land surface stations, ships and drifting buoys are used, as regulated by rejection lists. These rejection lists are updated monthly. In the absence of station pressure, mean sea level pressure is used. In the absence of both of these, the height of standard pressure levels (usually 850 or 700 hPa) may be used.

In situ upper air observations consist of temperatures, winds and relative humidity from radiosondes (TEMP messages), winds from PILOT balloons and wind profilers along with winds and temperatures from the Aircraft Meteorological Data Relay (AMDAR) and aircraft reports (AIREPS).

The bulk of the data processed by the OPS consists of information from infrared and microwave sounders aboard polar orbiting satellites. This includes the Advanced TIROS[1] Operational Vertical Sounder (ATOVS) data from the NOAA series of satellites. The assimilation system uses radiances from the High-resolution Infrared Radiation Sounder (HIRS/3), and Advanced Microwave Sounding Units A1, A2 and B, directly within the variational assimilation. The precise number of ATOVS channels varies with satellite, and is regularly upgraded to reflect variations in performance of the various sensors. The other source of sounder data is the Atmospheric Infra-Red Sounder (AIRS) aboard the NASA Earth Observing System satellite Aqua. Currently 62 channels are used from AIRS.

Finally, remotely sensed winds from scatterometers such as ASCAT and high density version Atmospheric Motion Vectors (AMVs) from geostationary imagery are also used.

The following is a summary of the observation types assimilated in the first operational implementation of ACCESS:

- Surface observations: synop, ship, profilers.
- Upper air observations: radiosondes, pilot balloons, wind profilers, AIREPS, AMDARS.
- Satellite winds: scatterometer surface winds, atmospheric vector winds.
- Microwave radiances: ATOVS (AMSU A, B and MHS).
- Infrared radiances: ATOVS (HIRS), AIRS.

Figure 2 provides an indication of the typical coverage of the different types of observations assimilated. It should be noted that ACCESS assimilates vastly increased number and types of observations, particularly satellite observations, compared to GASP and LAPS.

The next major upgrade of the system is scheduled to include other instruments such as the Infrared Atmospheric Sounding Interferometer (IASI) aboard the ESA MetOp series of satellites and occultation data from various global navigation satellite systems (GNSS) such as the Global Positioning System. Later upgrades will include microwave radiances from the SSMIS instrument, the differential delay in GNSS signals and high precision land-based receivers and eventually information from radars associated with precipitation, Doppler radial winds and information from microwave imagers.

Figure 3 provides an indication of the data flow in the ACCESS assimilation module.

Quality control

The first checks within the OPS involve comparisons against the model forecast as all observations are required to be within specified tolerances of the background. The tolerances are a function of both observation and background error variances. The background error variances are flow dependent, using a regression against smoothed fields.

There are also consistency (buddy) checks on the innovations (observation–background) for various observation types. For example, surface observations from land stations, ships and drifting buoys are compared against other surface observations; radiosondes and aircraft data are compared against each other and AMV's are compared with other AMV's. At this stage there is no check for time consistency of ship tracks.

Satellite sounders are subjected to a number of specific quality checks and adjustments. All sounder data are subjected to checks on window channels, a scan-dependent bias correction and a fixed version of the Harris and Kelly (2001) scheme using 850–300 hPa and 200–50 hPa thicknesses as the air-mass predictors. In addition a 1dVAR retrieval is attempted on each sounding as part of the quality control. The 1dVAR retrieval is the basis for sensor specific checks,

[1]TIROS is the Television InfraRed Observation Satellite

Fig. 2. Distribution of received and accepted observations (left and right hand panels respectively) for various observation types. From the top to bottom row: surface observations; radiosondes, profilers and pilots; aircraft; ATOVS; AIRS; atmospheric motion vectors and scatterometer

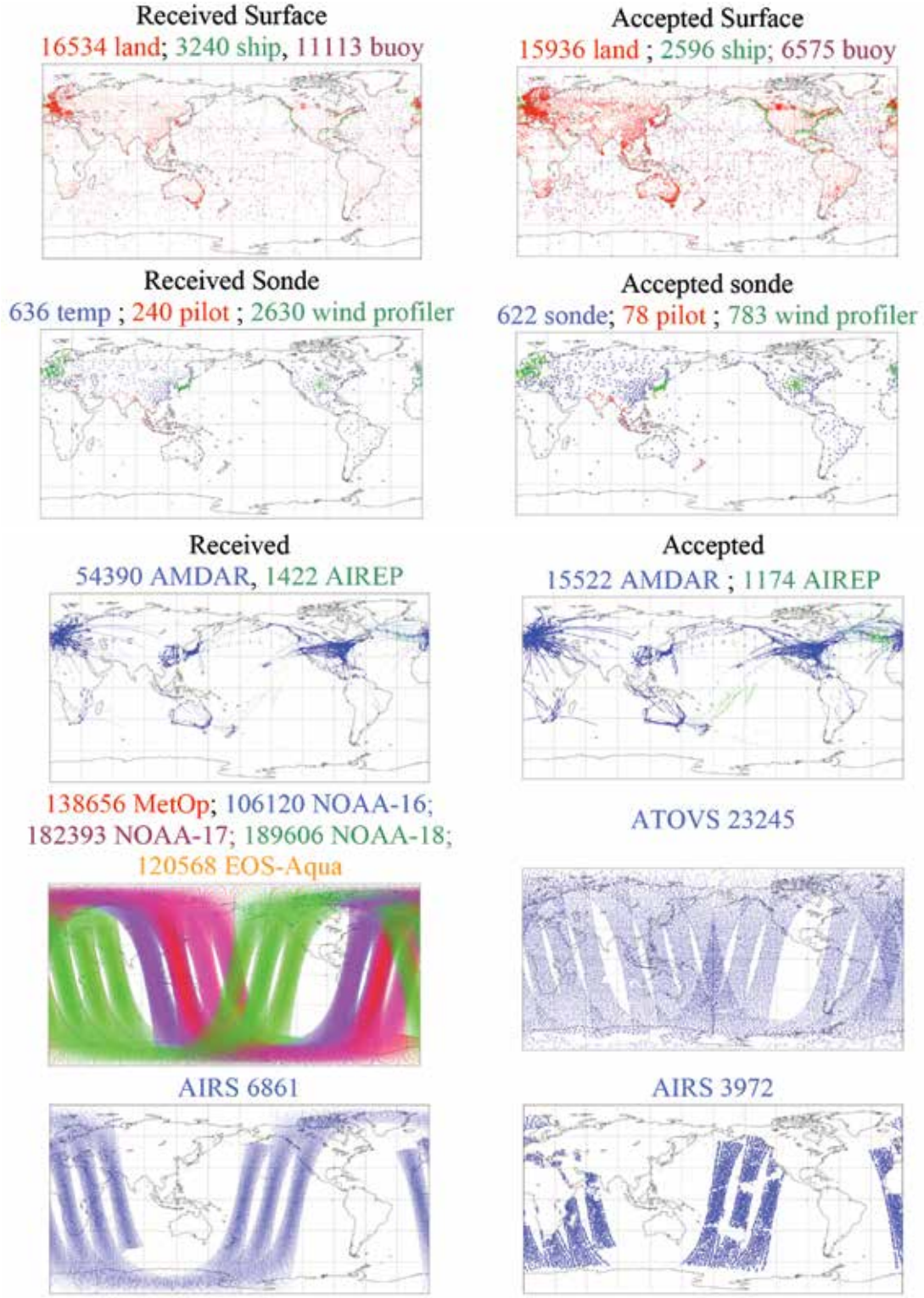

Fig. 2. continued.

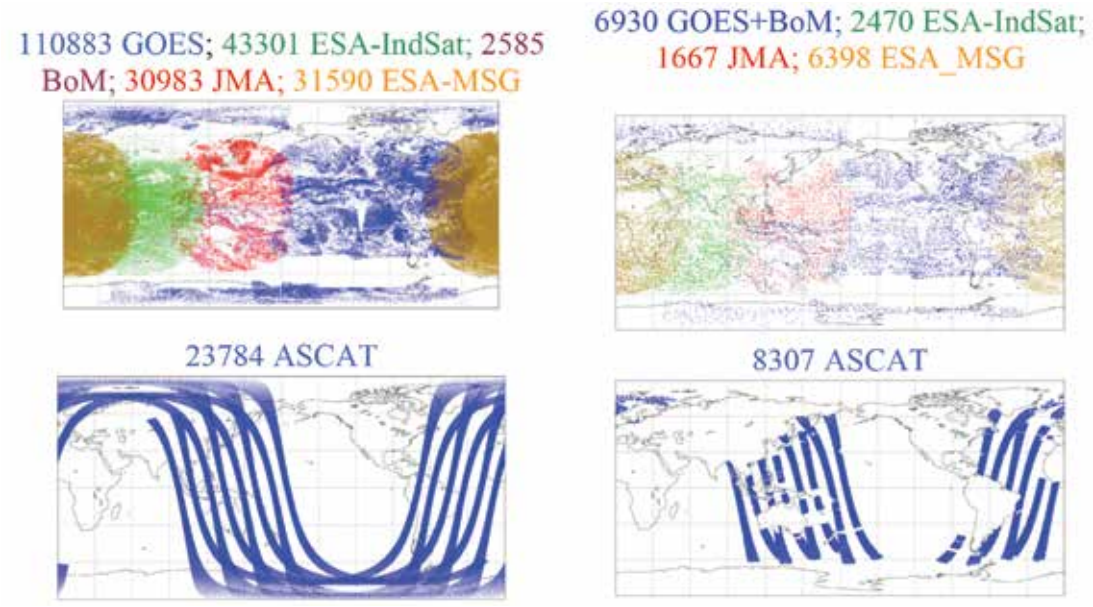

Fig. 3. Data flow in the ACCESS assimilation module. The dotted lines represent the flow of observation quality control and usage information back to the ODBs. This is not yet implemented.

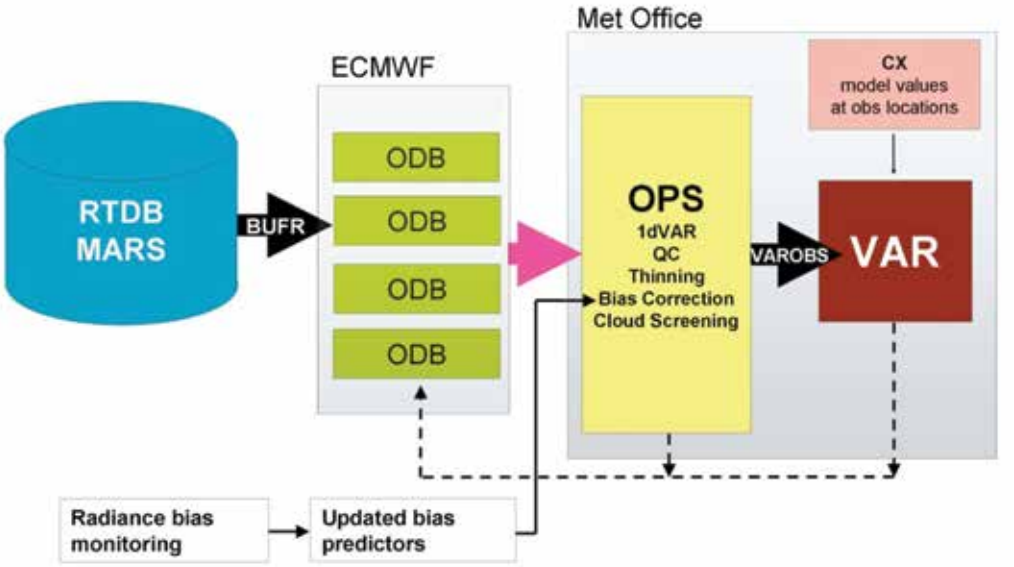

such as infrared cloud detection and cirrus and scattering index checks for the AMSU-B microwave channels.

All observations are thinned in space and time, with the degree of thinning being a function of model resolution.

Finally all observations are assigned a probability of gross error (PGE) which is adjusted during the variational minimisation. Observations where PGE > 0.5 are given zero weight. This variational adjustment of the PGE is very important for scatterometer data where the two leading ambiguities are provided to the variational analysis with the variational quality control then deciding which is most likely based on both the background and nearby observations (scatterometer data is also always rejected over sea-ice and land).

Variational assimilation

The assimilation system within the ACCESS NWP systems is an incremental 4-dimensional variational system. Details of this are provided in Rawlins et al. (2007) and references therein. This system allows for asynoptic observations to produce increments to the model initial conditions in a manner that is consistent with a linear perturbation forecast (or PF) model. The mass-wind balance is based on the linear balance equation. The PF model and therefore the increments are in terms of stream function, velocity

potential, unbalanced pressure and humidity.

The background error covariances are evaluated as a series of transforms: from the full model state variables to the PF state variables, followed by a vertical decomposition based on the projection onto the eigenmodes of the vertical error covariance matrix and a horizontal decomposition by either Legendre or double-sine transforms. An approximation is required to allow for the latitudinal variation of background error variances in the limited area model. While this approximation is not as accurate as on small domains, the size and location of ACCESS limited area domains, in particular ACCESS-R (see Table 2), which extends from 65°S to 14°N, make this approximation necessary.

Linear model and adjoint

The 4dVAR assimilation system requires a linear (PF) model to propagate the effects of increments to observation times, and an adjoint model to propagate the information within the innovations back to the initial time. The PF model uses semi-implicit semi-Lagrangian dynamics based on the UM, but is hydrostatic. The PF model also only contains very simplified physics with surface exchanges and vertical diffusion of momentum, heat and moisture via a modified Buizza (1994) scheme. Large-scale (resolved) precipitation is also included. More physical processes will be included in subsequent releases.

Initialisation

Previous NWP schemes have required some initialisation to rebalance the fields adjusted during the analysis step. This is a common feature amongst schemes using three-dimensional analysis techniques. The 4dVAR includes a balance term (J_c) in the cost function based on a digital filtering term using an 'elastic' energy norm, which measures the energy in the pressure perturbations. The digitally filtered field is taken as the weighted average of the perturbation fields across the assimilation window, from 15 to 345 minutes. The combination of the weak constraint, J_c and the strong constraint of the PF model provides very balanced increments and so no other initialization such as incremental analysis update or modal initialisation is required. This approach has the advantage that the balancing is performed in the presence of the observations, allowing for less adjustment in well observed areas and more adjustment in poorly observed areas.

In summary a broad outline of the 4dVAR algorithm at a nominal analysis time *T* is as follows:

1. Full field atmospheric forecasts from the UM are generated hourly between *T-3* and *T+3*.
2. The OPS selects observations within the window [*T-3*, *T+3*] which are then quality controlled.
3. Information on selected (thinned) observations and matching columns of background fields is generated providing all of the information for calculating observation-background differences (innovations).
4. The PF model runs from *T-3* to *T+3* storing the perturbations to the innovations.
5. The adjoint variables are initialised to zero and the adjoint model is run from *T+3* to *T-3* forced by the innovations (and the adjoint of the observation operator). This provides the gradient of the 4dVAR cost function with respect to the initial perturbation.
6. A suitable step is generated for use by a gradient-based minimisation algorithm to redefine the perturbation.
7. Steps 4–6 are repeated until a convergence or stopping criterion is satisfied.
8. The perturbations are converted from PF variables to full model variables and added to the first guess.

System architecture

Figure 4 shows a schematic of the NWP component of ACCESS and the Met Office systems. The key difference in the initial implementation of the ACCESS NWP system from the Met Office is the different computing environment, in particular the source of observational data, and the archive of forecast products. The ACCESS system has been interfaced into the Bureau's real-time stream of meteorological observations using the Observation Data Base (ODB) from the European Centre for Medium-range Weather Forecasts (ECMWF). This system provides a new set of files for each assimilation period that also generates a record of the observations presented to the operational suite. The ODB was chosen as it provides an efficient and flexible method for handling large amounts of data from a wide variety of sources, can store feedback statistics from assimilation, and has been implemented at a number of NWP centres. The operational archive of forecast products was also moved to the Meteorological Archive and Retrieval System (MARS), also from the ECMWF. This system has been shown to be an efficient archive and retrieval system well suited to use by modern NWP systems.

A further key difference in the NWP implementation is that the ACCESS suite uses the ECMWF SMS scheduler in

Fig. 4. Differences between the ACCESS and Met Office NWP systems.

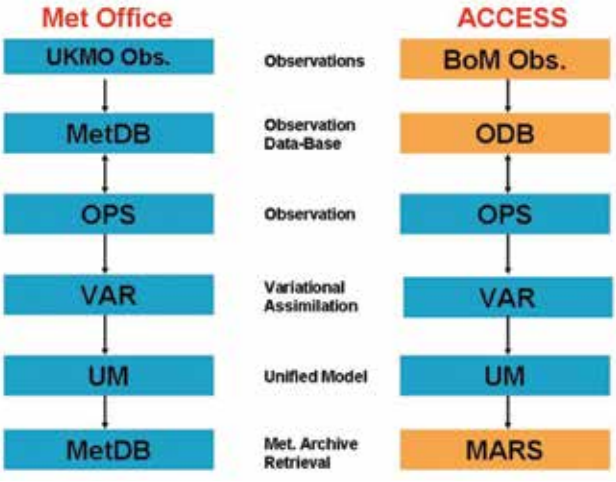

Table 2. Model domains and resolutions (in degrees, nominal distance equivalents and number of vertical levels) for initial (APS0) ACCESS implementation.

NWP system	*Domain*	*Resolution*	*Forecast duration (hours)*	*Forecast basetimes (UTC)*
ACCESS-G	Global	N144: 1.25° × 0.83° (80 km), L50	+240	00, 12
ACCESS-R	Regional	0.375° (37.5 km), L50	+72	00,06,12,18
ACCESS-A	Australia	0.11° (12.0 km), L50	+48	00,06,12,18
ACCESS-T	Tropical	0.375° (37.5 km), L50	+72	00, 12
ACCESS-C	Cities	0.05° (5 km), L50	+36	00, 12
ACCESS-TC	TC	0.11° (12 km), L50	+72	00, 12

the operational suite. The SMS scheduler has been used by NMOC for a long time and has many advantages over that used by the Met Office, who are planning to adopt a similar scheduling system for their modelling suites to replace their current suites software.

The Met Office practice of numbering pre-operational and operational parallel suites (as 'PS*n*') has been adopted for ACCESS NWP parallel suites. The initial operational ACCESS implementation is designated APS0 (Australian Parallel Suite 0). As shown in Table 2 and Fig. 13, APS0 retained the same model resolutions and configurations as the Bureau's previous global and regional NWP systems GASP and LAPS.

A key feature of the ACCESS systems is generation and archival of significant number of diagnostic products on model and pressure levels in addition to the standard model variables. Appendix A shows the comprehensive list of archived fields which should provide very useful information for researchers and forecasters.

Operational implementation

As noted above both global (ACCESS-G) and regional (ACCESS-R) systems became operational on the NEC SX6 supercomputer in September 2009 after detailed testing based on parallel runs extending over a year. The tropical region system (ACCESS-T; 0.375° × 0.375° × 50 levels) became operational in October 2009 and the high-resolution Australian region version (ACCESS-A) in June 2010. ACCESS-A was run in real time from September 2009 and operational adoption occurred after the Bureau's new SUN/Oracle supercomputer Solar was declared fully operational. In another key milestone, final operational switch over to solely running ACCESS-based systems on Solar occurred on 17 August 2010 with cessation of GASP and LAPS, followed by decommissioning of the NEC SX6 supercomputer. Further details of the operational implementation of ACCESS can be found in 'NMOC Operations Bulletin No. 83' (Bureau of Meteorology 2010).

Computational efficiency is very good with the global ACCESS-G system completing a full data assimilation and 240-hour forecast cycle within 35 minutes using 240 cores on the Solar supercomputer (the previous GASP system took over 115 minutes to complete its assimilation and forecast steps on the NEC SX6 supercomputer). Likewise, an ACCESS-R assimilation and 72-hour forecast cycle completes within 34 minutes using 160/80 cores for its assimilation/forecast steps (cf. 38 minutes for LAPS) and ACCESS-A completes within 75 minutes using 240/648 cores for its assimilation/forecast steps (cf. 82 minutes for MESOLAPS)

Some verifications

The ACCESS-based global and regional systems have resulted in a large improvement in skill relative to the Bureau's previously operational systems (GASP and LAPS). This is illustrated in Fig. 5 which shows the Australian Region S1 skill scores for the mean sea level pressure (MSLP) as a function of forecast time for ACCESS-R and LAPS, and for ACCESS-G and GASP, for the period 1 September 2009 to 30 June 2010; the figure also tabulates forecast gains (in hours) as a function of time. A key feature to note is the significantly increased skill of the ACCESS systems relative to the previously operational systems with forecast gains of ~24 hours for three-day forecasts. The MSLP verifications are representative of general skill as other variables at different levels show similar results. This can be clearly seen in Fig. 6 which shows the mean skill scores for 48-hour ACCESS-R and LAPS mean geopotential height forecasts as a function of height.

Verifications for ACCESS-A and ACCESS-T shown in Figs 7(a) and 7(b) again show significant gains in performance relative to the equivalent previous systems mesoLAPS, MALAPS and TXLAPS.

Additional forecast experiments have been run to identify whether the forecast improvement is due to improved forecast initial conditions from the data assimilation or differences in the forecast model. A sequence of hybrid forecasts was run with the UM forecast mode started from initial conditions from the GASP system. Figure 8 shows the skill of the hybrid forecasts (green) compared with GASP forecasts from GASP initial conditions (blue) and UM forecasts from UM initial conditions (red), verified in all three cases against operational GASP analyses. With the caveats that the conversion of the initial conditions may have had some negative impact on the hybrid forecasts, these results suggest that the forecast improvement is primarily

Fig. 5. Forecast gains as a function of forecast lead time for (i) upper panel: ACCESS-R (magenta) over LAPS (blue) and (ii) lower panel: ACCESS-G (magenta) over GASP (blue). The skill metric is S1 skill score for mean sea level pressure verified for the Australian region, averaged over the period 1 September 2009 to 30 June 2010.

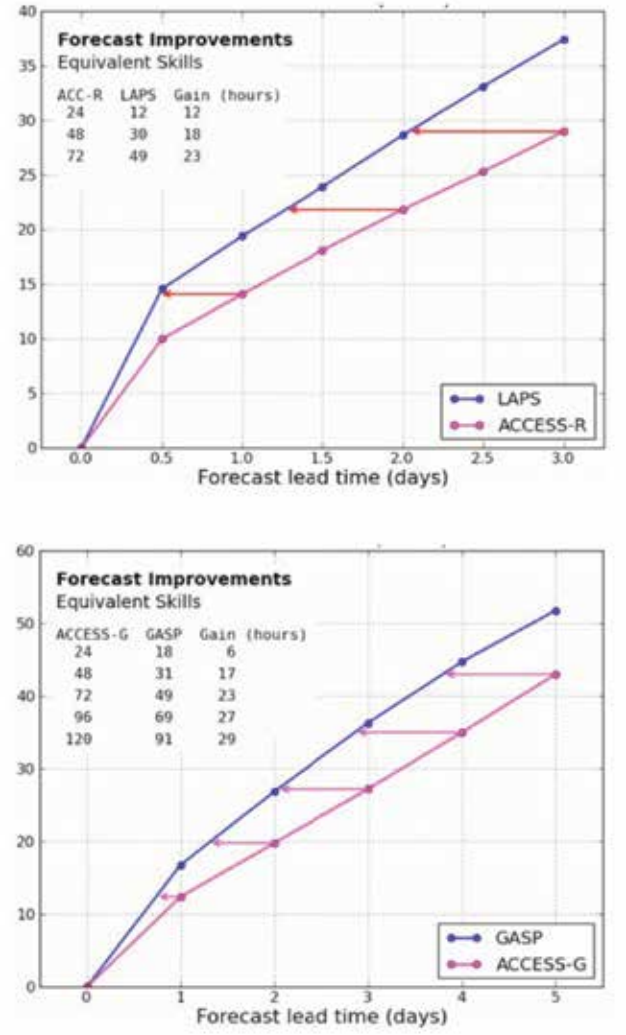

coming from the data assimilation improvement in the initial conditions.

Figure 9 shows a history of the performance of the Bureau's regional and global systems in terms of 12-month running mean of S1 skill score as a function of years. The global figure includes operational models from other international operational centres (ECMWF, MetOffice, NCEP and JMA). The figure shows a steady improvement in the Bureau models with large gains obtained through the implementation of LAPS and now ACCESS-R and ACCESS-G. As is clearly evident from the figure, over the past few years the performance of GASP had fallen significantly relative to the international global models. This performance gap has now been largely filled with the introduction of ACCESS-G. The slightly lower level of performance of ACCESS-G is attributed to its lower resolution relative to the other global models and the current usage of fewer satellite instruments.

Fig. 6. Mean S1 skill scores for 48-hour ACCESS-R mean geopotential height forecasts as a function of height (pressure) for the Australian region for the period 1 January 2010 to 30 June 2010 for LAPS (red) and ACCESS-R (green).

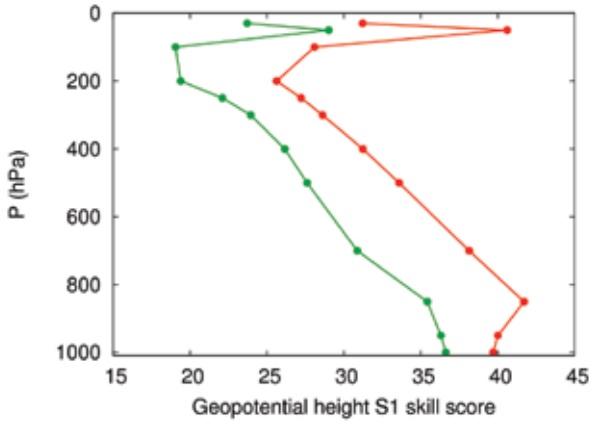

Fig. 7. (a) S1 skill scores of mean sea level pressure for ACCESS-A (green), MesoLAPS (red), and MALAPS (blue) as a function of forecast time for the period 5 November 2009 to 30 June 2010.

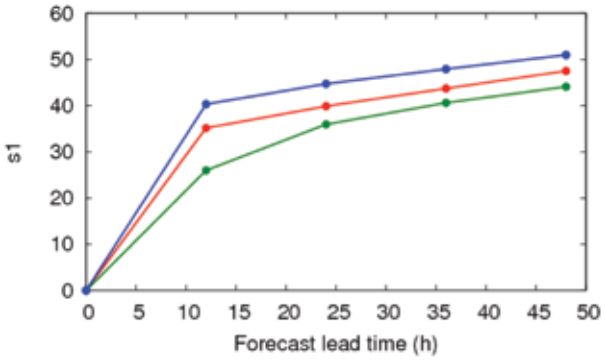

Fig. 7. (b) As in Fig. 6 but for rms errors for winds from ACCESS-T (green) and TXLAPS (red).

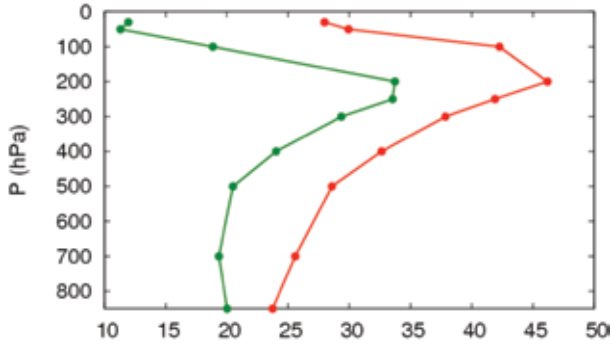

Figure 10 shows the January 2010 mean of 48-hour MSLP forecast errors for ACCESS-G and GASP. A key feature to note is the significantly lower biases over land areas for ACCESS-G. The mean June error (not shown) shows similar

Fig. 8. S1 skill scores of mean sea level pressure for hybrid UM model run from converted GASP initial conditions (green) compared to GASP model from GASP initial conditions (blue) and UM model from UM initial conditions (red). Skill scores are for the Australian region for a one month period in January 2007.

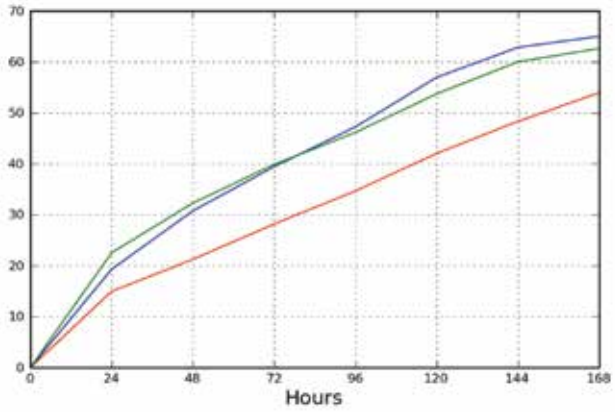

Fig. 9. History of performance of 48-hour forecasts from the Bureau's regional (top panel) and global (bottom panel) systems. The top panel includes LAPS (green) and ACCESS-R (red dot and triangle); the upper curve is for persistence. The bottom panel includes GASP (green), ACCESS-G (red dot) and global models from key international operational centres (ECMWF – red, MetOffice – maroon, NCEP – cyan and JMA – blue). The skill scores are for the Australian verification region.

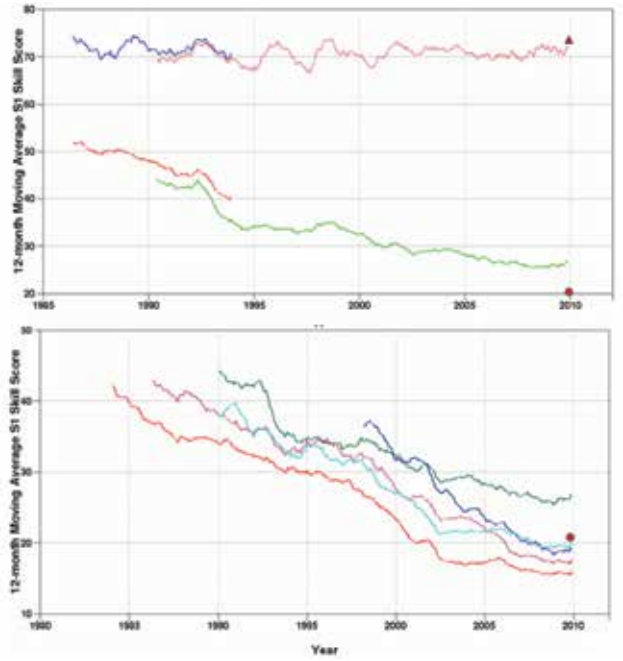

features.

Daily precipitation forecasts are of considerable interest to the public and pose considerable challenges for the forecasters. Tables 3 and 4 respectively show objective verifications for various measures of precipitation forecasts from ACCESS-R and LAPS and ACCESS-SY (Sydney region) and the corresponding LAPS Sydney region runs. The ACCESS-R verifications cover the period 1 September 2009 to 5 April 2010 while the ACCESS-SY cover a shorter period from 21 May 2010 to 19 June 2010.

Overall ACCESS-R is comparable or slightly better than LAPS in most scores for both time ranges, although ACCESS-R tends to under-do the average intensity and rain volumes whereas LAPS tends to overdo these. ACCESS-SY is comparable to or better than its LAPS counterpart (LAPS-SY) on most scores for both time ranges.

Some case studies

The following examples are shown to provide an indication of the potential of the ACCESS NWP systems to predict severe weather events that have high socio-economic impact. The years 2010 and 2011 were marked by severe flooding events over Victoria and Queensland. Both events caused flooding over very large regions in the two States. Thus, for example one-third of Victoria experienced some form of flooding while three-quarters of Queensland was declared a disaster zone, and the estimated cost of the floods in each State cost well over $1 billion. In Queensland a flash flood raced through Toowoomba's central business district resulting in loss of lives.

In early September 2010, significant flooding occurred across much of Victoria, when an extensive and slow-moving low pressure trough advected large amounts of moisture from tropical northern Australia over the State. The flooding was enhanced by orographic effects, particularly in northeastern Victoria. Figure 11 shows the observed rainfall for the 24-hour period from 9.00 am on 3 September to 9.00 am on 4 September 2010. Note the widespread heavy rain over a large part of Victoria. Figure 11 also shows the 72-hour, and 120-hour ACCESS-G mean sea level pressure (MSLP) and rainfall forecasts verifying at 0000 UTC 4 September 2010 together with the verifying MSLP analysis. Two features of note are (i) accurate model forecasts for the heavy rainfall up to five days ahead and (ii) very good consistency between the two forecasts; the 96-hour forecast (not shown) also showed similar consistency. The good consistency between forecasts starting from different initial conditions is an important feature that provides forecasters with greater confidence in providing medium-range forecasts of severe weather conditions. This was indeed the case for this event and very positive feedback about the performance of ACCESS was received from forecasters at the Victorian Regional Office who were responsible for providing the official forecasts.

In late January 2009, extreme heatwave conditions developed in southeastern Australia, exacerbated by a prolonged period of little or no rainfall. The unusually long

Fig. 10. Mean January MSLP 48-hour forecast error for ACCESS-G and GASP. Contour interval is 1 hPa, full (dashed) contour lines denote positive (negative) values.

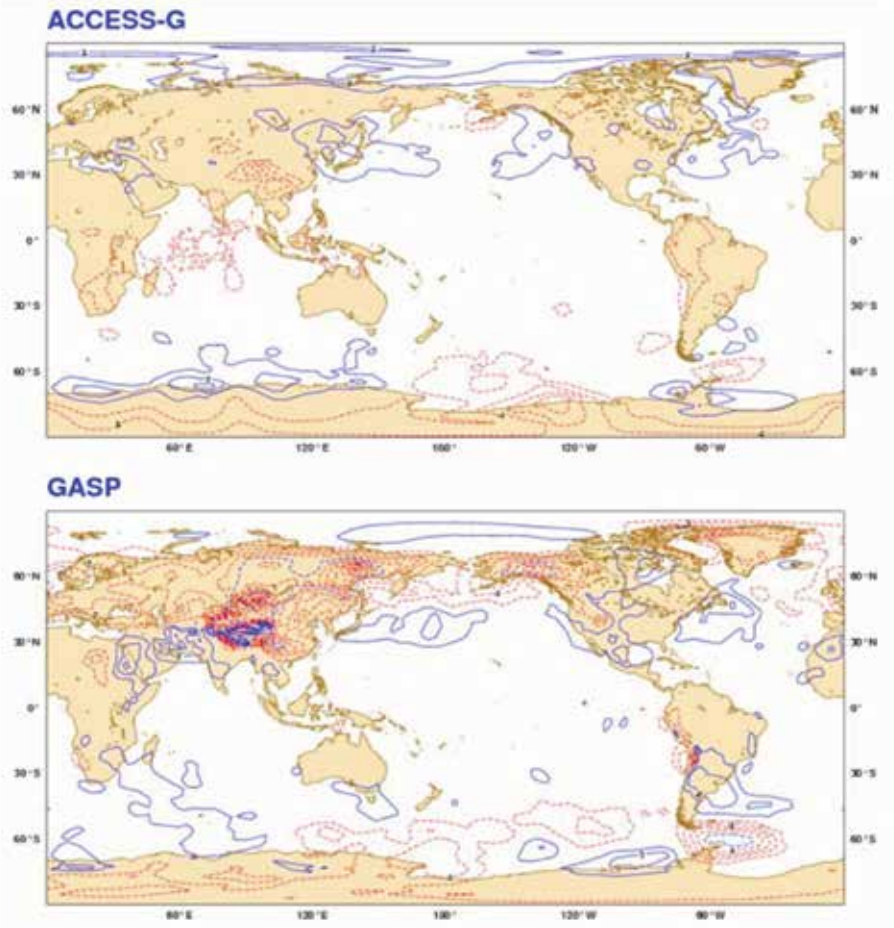

Table 3. Mean verification scores for precipitation forecasts (0–24 hours and 24–48 hours) from LAPS and ACCESS-R (blue – ACCESS better, red – ACCESS worse).

	Observed	*LAPS-R 00–24*	*ACCESS-R 00–24*	*LAPS-R 24–48*	*ACCESS-R 24–48*
Rain area ($km^2 \times 10^3$)	1204	1273	1297	1283	1261
Avg. intensity (mm/d)	11.14	11.82	8.21	11.14	8.07
Rain volume (km^3)	13.40	15.0	10.7	14.3	10.2
Max intensity (mm/d)	74.36	86.16	81.95	84.37	78.45
Mean abs. error (mm/d)		2.29	1.88	2.53	2.03
Average RMSE (mm/d)		6.34	5.51	6.92	5.93
Average correlation		0.54	0.55	0.45	0.50
Bias score		1.06	1.08	1.07	1.05
Probability of detection		0.72	0.74	0.68	0.70
False alarm ration		0.32	0.31	0.36	0.33
Critical success index		0.54	0.55	0.49	0.52
Hanssen and Kuipers score		0.63	0.65	0.58	0.61
Equitable threat score		0.45	0.47	0.39	0.43

Table 4. Mean verification scores for precipitation forecasts (0–24 hours and 24–36 hours) from LAPS-SY and ACCESS-SY (blue – ACCESS better, red – ACCESS worse).

	Observed	*LAPS-SY 00–24*	*ACCESS-SY 00–24*	*LAPS-SY 24–36*	*ACCESS-SY 24–36*
Rain area ($km^2 \times 10^3$)	120	81	106	86	103
Avg. intensity (mm/d)	8.58	10.18	7.97	10.89	8.29
Rain volume (km^3)	1.03	0.82	0.84	0.94	0.86
Max intensity (mm/d)	24.33	72.02	60.56	71.65	70.09
Mean abs. error (mm/d)		2.37	1.87	2.48	2.09
Average RMSE (mm/d)		5.00	3.69	5.23	4.10
Average correlation		0.43	0.55	0.44	0.52
Bias score		0.67	0.89	0.72	0.87
Probability of detection		0.62	0.77	0.65	0.75
False alarm ratio		0.08	0.13	0.10	0.13
Critical success index		0.59	0.69	0.45	0.68
Hanssen and Kuipers score		0.59	0.70	0.61	0.69
Equitable threat score		0.47	0.57	0.48	0.56

Fig. 11. Left panels: MSLP and 24-hour rainfall (mm) analyses valid for 0000 UTC 4 September 2010. Right panels: 72-hour (bottom) and 120-hour (top) forecasts also valid for 0000 UTC 4 September 2010.

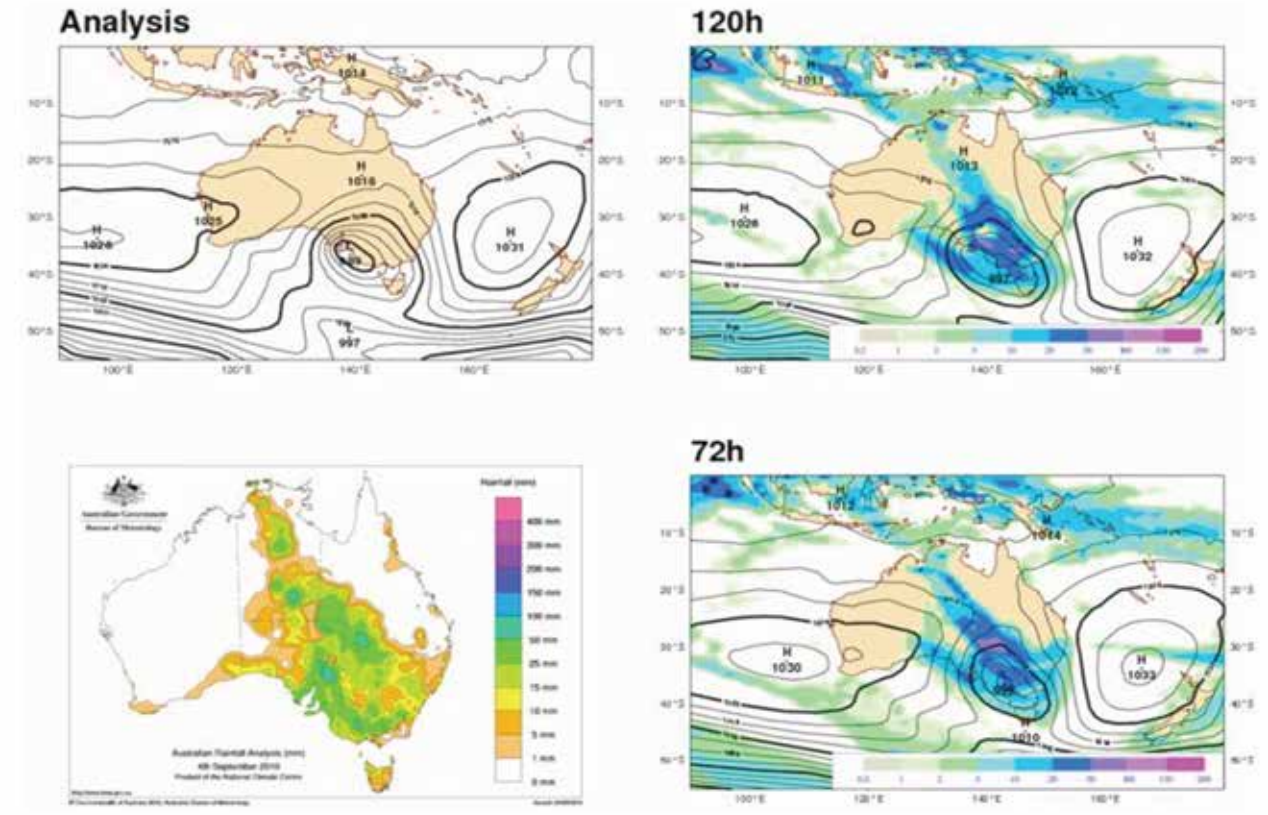

Fig. 12. 168-hour forecast from ACCESS-G valid for 0000 UTC 7 February 2009 (top right) and verifying analysis from ACCESS-G (top left) and NMOC (bottom left).

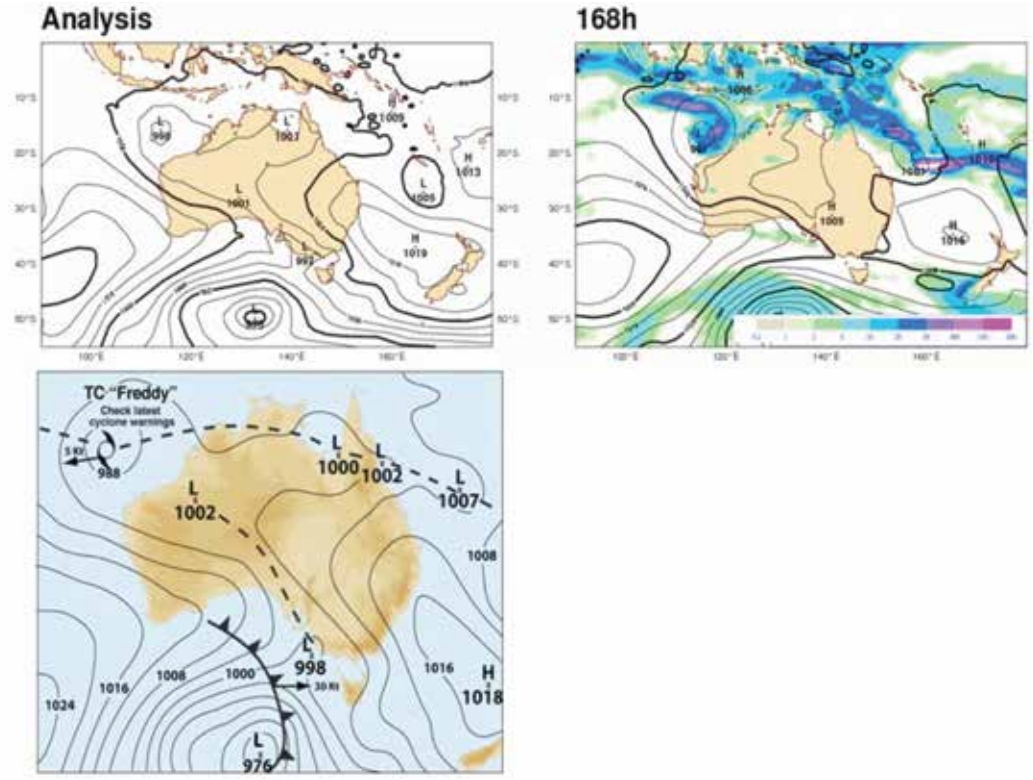

duration of the heatwave was associated with the development of a stable low pressure trough over much of the Australian continent. On 7 February 2009, record high temperatures were generated across much of Victoria as strong hot northerly winds developed ahead of an approaching cold front. As a result, Victoria experienced the worst fires in Australia's recorded history. The 'Black Saturday' fires claimed 173 lives and injured nearly 5000 people and burnt through nearly 4500 square kilometers of land. During the period a trial version of ACCESS-G was being run as part of detailed trials of the system prior to operational implementation. Figure 12 shows a 168-hour forecast valid for 0000 UTC on 7 February 2009 together with the ACCESS-G verifying analysis and the NMOC verifying analysis. Note the close agreement of the ACCESS analysis and the official NMOC analysis, and the good guidance of severe weather conditions (a high pressure system bringing hot northerly winds over Victoria and an impending cool change approaching) provided by the model seven days ahead.

ACCESS-G with a resolution of 80 km in the horizontal can only provide broad synoptic guidance for severe weather events. Much higher resolutions are essential to provide more detailed information to forecasters. A 3 km horizontal resolution limited area version of ACCESS was run in order to provide an indication of the potential of such a model for this case. Figure 13 shows the 12-hour, 18-hour, 23-hour (time of maximum temperature in southern Victoria) and 30-hour forecasts for vector winds at 10 m and temperatures at 2 m from this run. The model successfully simulates the strengthening northerly winds accompanied with rising temperatures (with maximum temperatures of over 45°C) followed by passage of a cool change in the evening within an hour of the observed time of the change.

Both examples indicate the considerable potential of the ACCESS global and regional (high resolution) NWP systems to provide detailed and useful guidance on severe weather events. It should be emphasised that it is only possible to present a small sample of cases in a paper such as this one. The cases shown are not isolated but provide an indication of the more general performance of the ACCESS-based NWP systems. Future plans for ACCESS development will focus on realising this potential more comprehensively.

Future development

Some recent extensions of the ACCESS NWP suite include the limited area tropical cyclone model (ACCESS-TC) which was implemented operationally in December 2012, ozone/UV prediction system and a limited area Antarctic version (ACCESS-P). All these extensions were developed in collaboration with CAWCR's Weather and Environmental Prediction program. Additionally a number of ACCESS-based downstream systems such as the atmospheric transport model based on HYSPLIT have been developed.

The design of ACCESS, which is consistent with seamless prediction, provides a platform that allows the flexibility

Fig. 13. 12, 18, 23 and 30-hour forecasts from 0600 UTC 6 February 2009 for vector winds at 10 m and temperatures at 2 m from an experimental limited area ACCESS model run with 3 km resolution in the horizontal and 50 vertical levels.

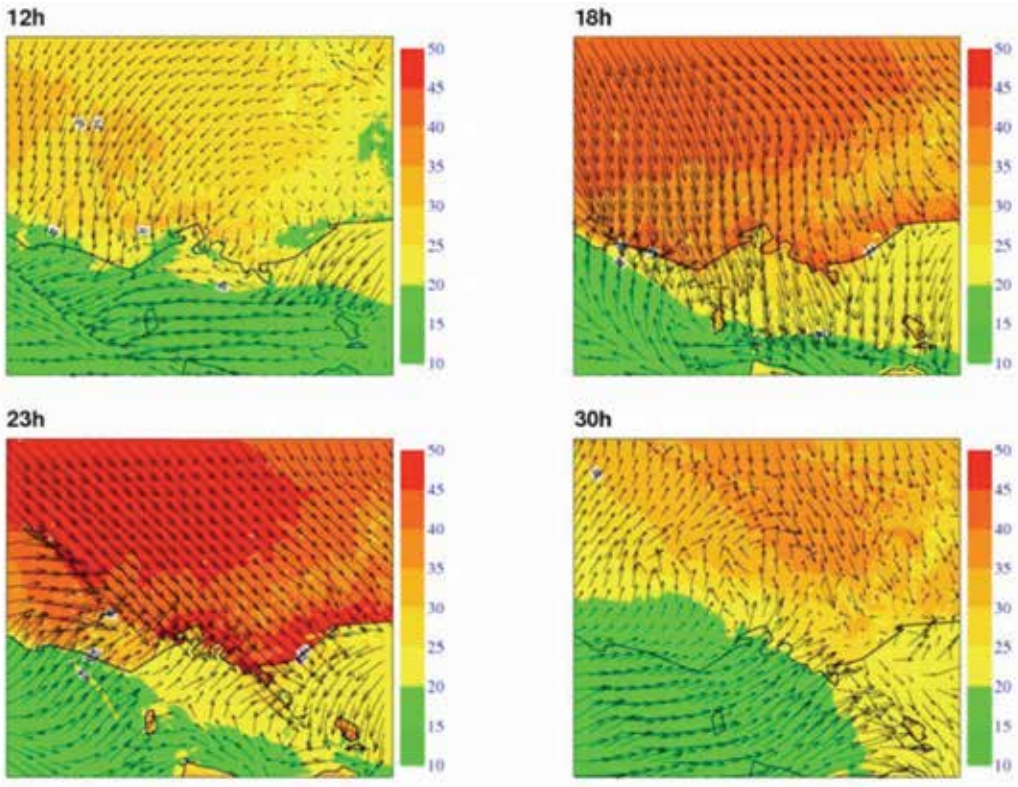

needed to implement major upgrades and new applications. Thus for example the non-hydrostatic formulation readily allows increased resolutions and 4dVAR allows assimilation of data from a wide variety of platforms including significantly enhanced sounders planned for new satellite launches.

An ongoing activity at major operational centres is regular upgrades to the operational systems. The upgrades include improved numerics, improved physical parametrisations, developments in analysis formulations, and assimilation of new sources of data particularly from new satellite sounders. This ongoing work has been essential to realise the major improvements in numerical weather prediction over the past decade. The ACCESS NWP system will need to follow this practice of regular upgrades if its forecast performance is to remain competitive with that of other international centres. Accordingly, planning for the next upgrades (APS1 and APS2) has commenced. The first upgrade, APS1, planned for implementation in 2012 will include increased resolutions (N320 (40 km) 70 levels for ACCESS-G and 12 km 70 levels for ACCESS-R) while the second upgrade, APS2, planned for 2014 will include further increases in resolution (N512 (25 km) 70–90 levels for ACCESS-G, and 2–3 km for ACCESS-C). The upgrades will also include improvements to physical parametrisations, assimilation of wider variety of satellite sounders (e.g. IASI and GPS data and use of cloudy radiances), and a rationalisation of the regional domains (see Fig. 14). The upgrades to the NWP suite will also include routine experimental running of the 24 member ACCESS global and regional ensemble prediction systems, AGREPS.

A major challenge facing weather prediction centres is reduction and mitigation of adverse effects of weather. In response to this there has been a major shift in emphasis towards severe weather prediction. Australia is vulnerable to the ravages of adverse weather such as tropical cyclones, high rainfall, high winds, fire-weather conditions etc. Tropical cyclones, for example, represent the most regular major natural meteorological disaster affecting the tropical regions of the southern hemisphere and result in major socio-economic impact. Thus a major emphasis in the future development of ACCESS NWP will be in severe weather prediction and research. This development will be closely tied to AGREPS that is being run routinely in research mode for global and regional configurations, and the Strategic Radar Enhancement Project (SREP), which involves a new research effort in high resolution NWP assimilation of radar precipitation and wind data, as well as the installation of four Doppler radars.

Conclusion

ACCESS has made significant progress since its start in 2005, with operational implementation of the ACCESS-based NWP systems by the Bureau, successful assembly of the fully-coupled ACCESS model, and execution of core runs to be submitted for the IPCC Fifth Assessment

Fig. 14. ACCESS NWP domains for suites APS0 and APS1.

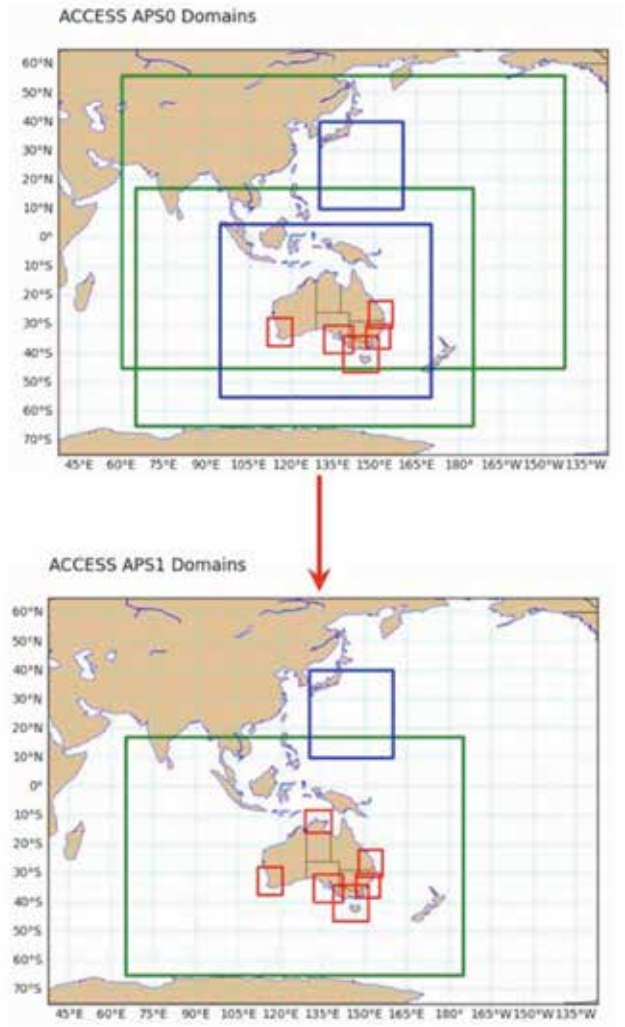

Report. Significant progress has been made with ACCESS infrastructure. Examples include successful porting to both Solar and Vayu (NCI) machines, development of infrastructure to allow usage by university researchers and setting up of a unified inventory based at NCI. A pleasing aspect is the increasing use of ACCESS by researchers, including experimentation with physical parametrisations, tropical cyclone studies, impact of enhanced stratospheric resolution, use of idealised limited area version of ACCESS, and atmospheric tracer mass conservation in the UM.

As noted above the design of ACCESS provides a platform that has the flexibility needed to implement major upgrades and new applications. The results obtained from the initial operational implementation, including major performance gains relative to the Bureau's previously operational systems (GASP and LAPS), provide considerable confidence that future upgrades will deliver continuing substantial improvements in the Bureau's ability to provide forecasts of increasing precision and reliability, and support for researchers' efforts to understand the meteorology of the Australian region.

Acknowledgements

The atmospheric model (UM) and data assimilation (4dVAR) used in the ACCESS NWP suite were developed at the Met Office. The continuing and timely support and advice on UM and 4dVAR by Met Office staff is gratefully acknowledged. ACCESS NWP implementations would not have been possible without this support. We are grateful for support and feedback from colleagues in CAWCR's Earth System Modelling, Weather and Environmental Prediction and Atmosphere–Land Observation and Assessment Programs, and the Bureau's National Meteorological and Oceanographic Centre.

References

Arakawa, A. and Lamb, V.R. 1977. Computational design of the basic dynamical processes of the UCLA general circulation model. *Methods in Comp. Phys., 17,* 174–265.

Bermejo, R. and Staniforth, A. 1992. The conversion of semi-Lagrangian advection schemes to quasi-monotone schemes. *Mon. Wea. Rev., 120,* 2622–32.

Best, M. and Maisey, P. 2002. A physically based soil moisture nudging scheme. Hadley Centre technical note 35, Met. Office, Exeter, UK.

Bi, D., Dix, M., Marsland, S.J., O'Farrell, S., Rashid, H., Uotila, P., Hirst, A., Kowalczyk, E., Golebebiewski, M., Sullivan, A., Hailin, Y., Hannah, N., Franklin, C., Sun, Z., Vohralik, P., Watterson, I., Zhou, X., Fiedler, R., Collier, M., Noonan, J., Stevens, L., Uhe, P., Zhou, X., Hill, R., Harris, C., Griffies, S., and Puri, K. 2013, The ACCESS coupled model: description, control climate and evaluation. *Aust. Met. Oceanogr. J., 63,* 41–64.

Buizza, R. 1994. Sensitivity of optimal unstable structures. *Q. J. R. Meteorol. Soc., 120,* 429–51.

Bureau of Meteorology. 2010. Operational implementation of the ACCESS Numerical Weather Prediction systems. NMOC Operations Bulletin No. 83. Accessible via http://www.bom.gov.au/nwp/doc/bulletins/apob83.pdf

Bushell, A.C., Scaife, A.A., and Warner, C.D. 2007. Non-Orographic (Spectral) Gravity Wave Parameterization, Unified Model Documentation Paper No. 34.

Campbell, G. 1974. A simple method for determining unsaturated conductivity from moisture retention data. *Soil Science, 117,* 311.

Charney, J.G., and Phillips,N. A. 1953. Numerical integration of the quasi-geostrophic equations for barotropic and simple baroclinic flows. *J. Meteor., 10,* 71–99.

Clark, T.L. 1977. A small-scale dynamic model using a terrain-following coordinate transformation. *J. Comput. Phys., 24,* 186–215.

Cosby, B., Hornberger, G., Clapp, R., and Ginn, T. 1984. A statistical exploration of the relationships of soil moisture characteristics to the physical properties of soils. *Water Resources Research, 20,* 682–90.

Cox, P., Betts, R., Bunton, C., Essery, P., Rowntree, R., and Smith, J. 1999. The impact of new land surface physics on the GCM simulation of climate and climate sensitivity. *Clim. Dyn., 15,* 183–203.

Cullen, M.J.P. 1993. The unified forecast/climate model. *Meteor. Mag., 122,* 81–94.

Davies, T., Cullen, M.J.P., Malcolm, A.J., Mawson, M.H., Staniforth, A., White, A.A., and Wood, N. 2005. A new dynamical core for the Met Office's global and regional modelling of the atmosphere. *Q. J. R. Meteorol. Soc., 131,* 1759–82.

Edwards, J., and Slingo A. 1996. Studies with a flexible new radiation code. I: choosing a configuration for a large-scale model. *Q. J. R. Meteorol. Soc., 122,* 689–719.

Edwards, J.M., Beare, R.J., and Lapworth, A.J. 2006. Simulations of the observed evening transition and nocturnal boundary layers: Single-column modelling. *Q. J. R. Meteorol. Soc., 132,* 61–80.

Edwards, J., Havemann, S., Thelen, J.-C., and Baran A.J. 2007. A new parameterization for the radiative properties of ice crystals: Comparison

with existing schemes and impact in a GCM. *Atmospheric Research, 83,* 19–35, doi:10.1016/j.atmosres.2006.03.002.

Essery, R., Best, M., and Cox, P. 2001. MOSES 2.2 technical documentation. Hadley Centre technical note 30, Met. Office, Exeter, UK.

Gregory, D., and Rowntree P.R. 1990. A mass flux convection scheme with representation of cloud ensemble characteristics and stability-dependent closure. *Mon. Weather Rev., 118,* 1483–506.

Harris, B.A. and Kelly G. 2001. A satellite radiance-bias correction scheme for data assimilation. *Q. J. R. Meteorol. Soc., 127,* 1453–68.

King, J.C., Connolley, W.M., and Derbyshire S.H. 2001. Sensitivity of modelled Antarctic climate to surface and boundary-layer parametrizations. *Q. J. R. Meteorol. Soc., 127,* 779–94.

Laprise R. 1992. The Euler Equations of motion with hydrostatic pressure as independent variable. *Mon. Wea. Rev., 120,* 197–207.

Lock A.P., Brown, A.R., Bush, M.R., Martin, G.M., and Smith R.N.B. 2000. A new boundary layer mixing scheme. Part I: Scheme description and single-column model. *Mon. Weather Rev., 128,* 3187–99.

Louis, J.F. 1979. A parametric model of vertical eddy fluxes in the atmosphere. *Bound. Lay. Met., 17,* 187–202.

McDonald, A. and Bates, J.R. 1989. Semi-Lagrangian integration of a gridpoint shallow water model on the sphere. *Mon. Wea. Rev., 117,* 130–7.

McFarlane, N.A. 1987. The effect of orographically excited gravity wave drag on the General Circulation of the lower stratosphere and troposphere. *J. Atmos. Sci., 44,* 1775–800.

Rawlins, F., Ballard, S.P., Bovis, K.J., Clayton, A.M., Li, D., Inverarity, G.W., Lorenc, A.C., and Payne, T.J. 2007. The Met Office global four-dimensional variational data assimilation scheme. *Q. J. R. Meteorol. Soc., 133,* 347–62.

Ritchie, H. and Beaudoin, C. 1994. Approximations and sensitivity experiments with a baroclinic semi-Lagrangian spectral model. *Mon. Wea. Rev., 122,* 2391–9.

Rivest, C., Staniforth, A. and Robert, A. 1994. Spurious resonant response of semi-Lagrangian discretizations to orographic forcing: diagnosis and solution. *Mon. Wea. Rev., 122,* 366–76.

Scaife, A.A., Butchart, N., Warner, C.D., Stainforth, D., Norton, W., and Austin, J. 2000. Realistic Quasi-Biennial Oscillations in a simulation of the global climate. *J., Geophys. Res., 27,* 3481–4.

Scaife, A.A., Butchart, N., Warner, C.D. and Swinbank, R. 2002. Impact of a spectral gravity wave parameterization on the stratosphere in the Met. Office Unified Model. *Q. J. R. Meteorol. Soc., 59,* 1473–89.

Smith, R.N.B. 1990. A scheme for predicting layer clouds and their water contents in a general circulation model. *Q. J. R. Meteorol. Soc., 116,* 435–60.

Staniforth, A., White, A., Wood, N., Thuburn, J., Zerroukat, M., Cordero, E., Davies, T., and Diamantakis, M. 2006. Unified Model Documentation Paper No 15: Joy of U.M. 6.3 – Model Formulation. Available at: http://research.metoffice.gov.uk/research/nwp/publications/papers/unified_model/umdp15_v6.3.pdf

Walters, D.N., Best, M.J., Bushell, A.C., Copsey, D., Edwards, J.M., Falloon, P.D., Harris, C.M,. Lock, A.P., Manners, J.C., Morcrette, C.J., Roberts, M.J., Stratton, R.A., Webster, S., Wilkinson, J.M., Willett, M.R., Boutle, I.A., Earnshaw, P.D., Hill, P.G., MacLachlan, C., Martin, G.M., Moufouma-Okia, W., Palmer, M.D., Petch, J.C., Rooney, G.G., Scaife, A.A. and Williams, K.D. 2011. The Met Office Unified Model Global Atmosphere 3.0/3.1 and JULES Global Land 3.0/3.1 configurations. *Geosci. Model Dev., 4,* 919–41

Warner, C.D., Scaife, A.A., and Butchart, N. 2005. Filering of parameterized nonorographic gravity waves in the Met Office Unified Model. *J. Atmos. Sci., 62,* 1831–48.

Warner, C.D. and McIntyre, M.E. 1996. On the Propagation and Dissipation of Gravity Wave Spectra through a Realistic Middle Atmosphere. *J. Atmos. Sci., 53,* 3213–35.

Warner, C.D. and McIntyre, M.E. 1999. Towards an ultra-simple spectral gravity wave parameterization for general circulation models. *Earth, Planets and Space, 51,* 475–84.

Warner, C.D. and McIntyre, M.E. 2001. An Ultrasimple Spectral Parameterization for Nonorographic Gravity Waves. *J. Atmos. Sci., 58,* 1837–57.

Webster, S. 2004. Gravity Wave Drag. Unified Model Documentation Paper No. 22, Met Office, Exeter, UK

Webster, S., Brown, A.R., Cameron, D.R. and Jones, C.P. 2003. Improvements to the representation of orography in the Met. Office Unified Model. *Q. J. R. Meteorol. Soc., 129,* 1989–2010.

Wilson, D.R. and Ballard, S.P. 1999. A microphysically based precipitation scheme for the UK Meteorological Office Unified Model. *Q. J. R. Meteorol. Soc., 125,* 1607–36.

Wilson, M. and Henderson-Sellers, A. 1985: A global archive of land cover and soils data for use in general circulation climate models. *J. Climatol., 5,* 119–143.

Appendix A

Table A1. Table of model level output fields

Standard Name	*GRIB ID*	*Units*	*STASH No.*	*STASHMASTER Name*
soil_mois	140.128	m	8223	Soil moisture content in a layer
soil_temp	139.128	K	8225	Deep soil temp. after hydrology
height_theta	138.228	m	15101	Height of theta model levs from sea level
height_rho	139.228	m	15102	Height of rho model levs from sea level
air_temp	130.128	K	16004	Air temperature on theta levels
zonal_wnd	131.128	m/s	2	Zonal component of wind after time step
merid_wnd	132.128	m/s	3	Meridional component of wind afte time step
spec_hum	133.128	kg/kg	10	Specific humidity after time step
omega	135.128	Pa/s	150	Vertical component of wind after time step
p_half	55.128	Pa	407	Pressure at rho levels after time step
pressure	54.128	Pa	408	Pressure at theta levels after time step
conv_cldtop_pres	90.128	Pa	5208	Pressure at convective cloud top
conv_cldbse_pres	89.128	pa	5207	Pressure at convective cloud base
conv_cld	185.128	%	5212	Convective cloud amount on each model lev
conv_cld_water	88.128	kg/kg	5213	Convective cloud condensed water
cld_ice	247.128	kg/kg	12	Frozen cloud condensate mixing ration after time step
cld_water	246.128	kg/kg	254	Liquid cloud condensate mixing ratio after time step
area_cld_frac	82.128	–	265	Area cloud fraction in each layer
lqd_cld_frac	83.128	–	267	Liquid cloud fraction in each layer
ice_cld_frac	84.128	–	268	Frozen cloud fraction in each layer

Table A2. Table of single-level output fields

Standard Name	*GRIB ID*	*Units*	*STASH No.*	*STASHMASTER Name*
accum_prcp	61.228	mm	5226	Accumulated total precipitation amount
av_netswsfc	212.228	W/m^2	1201	Mean net down surface sw flux after time step
av_swirrtop	216.228	W/m^2	1207	Mean incoming sw rad flux (toa): all tss
av_swsfcdown	214.228	W/m^2	1235	Mean total downward surface sw flux
av_sfc_sw_dir	115.228	W/m^2	1330	Mean direct downward sw flux at sfc
av_sfc_sw_dif	47.228	–	1331	Mean diffuse downward sw flux at sfc
av_netlwsfc	211.228	W/m^2	2201	Mean net down surface lw rad flux
av_olr	215.228	W/m^2	2205	Mean outgoing lw rad flux (toa)
av_lwsfcdown	213.228	W/m^2	2207	Mean downward lw rad flux: surface
accum_ls_prcp	142.228	mm	4201	Accumulated large scale rain amount
accum_ls_snow	240.228	mm	4202	Accumulated large scale snow amount
uwnd10m	165.128	m/s	3209	10 metre wind u-comp
av_uwnd10m	233.228	m/s	3209	Mean 10 metre wind u-comp
vwnd10m	166.128	m/s	3210	10 metre wind v-comp
av_vwnd10m	234.228	m/s	3210	Mean 10 metre wind v-comp
sens_hflx	146.128	W/m^2	3217	Surface heat flux
av_sens_hflx	222.228	W/m^2	3217	Mean surface heat flux
accum_evap	57.228	mm	3229	Accumulated evap from soil surf
lat_hflx	147.128	W/m^2	3234	Surface latent heat flux
av_lat_hflx	221.228	W/m^2	3234	Mean surface latent heat flux
temp_scrn	167.128	K	3236	Temperature at 1.5 m

Standard Name	*GRIB ID*	*Units*	*STASH No.*	*STASHMASTER Name*
tmax_scrn	201.128	K	3236	Maximum temperature at 1.5 m
av_temp_scrn	200.228	K	3236	Mean temperature at 1.5 m
tmin_scrn	202.128	K	3236	Minimum temperature at 1.5 m
qsair_scrn	81.128	kg/kg	3237	Specific humidity at 1.5 m
av_qsair_scrn	253.228	kg/kg	3237	Mean specific humidity at 1.5 m
dewpt_scrn	168.128	K	3250	Dewpoint at 1.5 m
uwnd_strs	180.128	$N/m^2/s$	3460	X-comp surface bi stress
av_uwnd_strs	224.228	pa	3460	Mean x-comp surface bi stress
vwnd_strs	181.128	$N/m^2/s$	3461	Y-comp surface bi stress
av_vwnd_strs	225.228	pa	3461	Mean y-comp surface bi stress
fric_vel	126.228	m/s	3465	Friction velocity
accum_conv_prcp	143.228	mm	5201	Accumulated convective rain amount
accum_conv_snow	239.228	mm	5202	Accumulated convective snow amount
soil_mois_cont	86.128	–	8208	Soil moisture content
canopy_wtr_cont	87.128	–	8209	Canopy water content
low_cld	186.128	%	9203	Low cloud amount
mid_cld	187.128	%	9204	Medium cloud amount
hi_cld	188.128	%	9205	High cloud amount
ttl_cld	164.128	%	9217	Total cloud amount max/random.overlp
av_ttl_cld	217.228	%	9217	Mean total cloud amount max/random overlp
mslp	151.128	hPa	16222	Pressure at mean sea level
av_mslp	202.228	hPa	16222	Mean pressure at mean sea level
sfc_temp	125.128	K	24	Surface temperature after time step
abl_ht	159.128	m	25	Boundary layer depth after time step
veg_ruff	109.128	m	26	Roughness length after time step
sea_lnd_mask	172.128	0/1	30	Land mask (no halo) (land = true)
seaice	31.128	0/1	31	Fraction of sea ice in sea after time step
sfc_geop	129.128	m	33	Orography
sfc_pres	134.128	Pa	409	Surface pressure after time step